JOURNAL OF CATALYSIS 67, 392–401 (1981)

Measurement of Effective Binary Gas Diffusion Coefficients in Porous Catalysts

L. G. GIBILARO AND S. P. WALDRAM

Department of Chemical and Biochemical Engineering, University College London, Torrington Place, London WC1E 7JE, England

Received February 27, 1980; revised May 28, 1980

The advantages of evaluating an effective diffusion coefficient from a transient concentration test involving only a single porous pellet are discussed. For real commercial catalysts it may be impossible to produce accurate results with a single pellet and in this case several pellets housed in a purpose-built cell can be tested. Experimental results for such an arrangement are presented. For cylindrical pellets these tests can also be used to detect anisotropy within the pellet structure. Results are for binary diffusion of argon and nitrogen in Hydronyl 356 GA 4C alumina pellets, and involve a carefully engineered apparatus. Effective diffusivities calculated from system moments are generally reproducible to within ±12% and average values for the diffusivities in radial and axial directions within the pellet agree to within ±25%. Pellet voidages, also determined from the moments, are consistent with independent measurements of the same.

INTRODUCTION

It is extremely difficult to manipulate real systems into forms for which relatively simple mathematical models are an adequate description; conversely, really complex models which are intended to mimic closely particular physical systems are frequently so cumbersome that their application and solution becomes impossible. In this article we employ a simple model to describe transient diffusion within a porous pellet and outline the steps taken to ascertain that this model is still an adequate description of a particular experimental system. Far more complicated mathematical descriptions of diffusion within porous solids abound, but the ability of these models to interpret real experimental data is usually limited; often too many unknown, or inaccurately known, parameters are present and the experiment can seldom be conducted with sufficient accuracy or discrimination to define them. As in so many areas of engineering, an enormous gulf separates the theoretician from the practitioner concerned with real process systems. There is clearly a demand for a simple, fast method to evaluate meaningful effective diffusivities in porous solids and the purpose of this paper is to outline a method which could fulfil this need.

Effective diffusivities can be required for several reasons: they may be needed so that during catalyst formulation active species can be laid down precisely or with specified concentration profiles on a porous matrix or support; in experimental work on heterogeneous reactions an effective diffusivity will be needed to check the value of the Wagner modulus (*1*) and hence determine the intrinsic reaction kinetics; finally in reactor design the diffusivity will be needed to evaluate the Thiele modulus, which can then be an aid in predicting reaction rates for heterogeneous systems. In addition a simple and quick testing method could be used as a screening or quality control procedure during catalyst manufacture.

Experimental methods for measuring binary gas diffusion coefficients within porous solids fall into several well-defined groupings. Early tests were *steady state* in character and involved sealing a single cylindrical pellet, usually of a catalyst, over

0021-9517/81/020392-10$02.00/0

its curved surface and allowing separate gas streams to flow past each flat end face (*2*). Experimental conditions were chosen to minimise both mass transfer resistances at the exposed surfaces and convective flow through the pellet; effective diffusivities were found by monitoring the pickup of one gas stream in the other, normally by means of a chromatographic technique. Many variations on the basic theme have been developed but it remains the essential ingredient of all steady-state methods. However, due to the confined geometrical circumstances necessarily imposed by such techniques the results reflect only the flux through the major pores which interconnect the flat end faces of the pellet and are therefore of little relevance to real applications. Furthermore the tests cannot reflect the presence of any dead-ended or laterally distributed microporous structure around the major pores and it is here where the major part of the activity of the solid is likely to lie. The tests can be criticised on further counts, two of the most important being that for commercial pellets the sealing over the curved surface, or the housing in some type of purpose-built leak-free mount, cannot easily be achieved, nor can anisotropy studies be readily conducted. Attempts to assess the degree of anisotropy within the structure would involve machining the pellet in some fashion, a process which in itself may well modify the surface structure and hence affect the results. No doubt some of these reasons have forced experimenters to study fairly large purpose-pressed pellets rather than real industrial catalysts, though Weisz (*3*) cleverly adapted the original apparatus to allow testing of commercial catalysts of either cylindrical or spherical form.

Unsteady-state testing techniques have become increasingly popular, and first we consider those conducted on a *single pellet*. Unsteady-state tests are generally more difficult to conduct and extract information from than their steady-state counterparts and this is a major disadvantage. Conversely, there are characteristics which make such tests attractive, amongst the most important of which are that all the pores influence the result and the severe geometric constraints necessarily imposed for the steady-state tests become unnecessary. Curiously the many investigators who have conducted such tests have seldom exploited this latter advantage, usually employing an experimental apparatus identical or very similar to that used for the steady-state runs and introducing a pulse of a diffusing species at one face of the pellet (*4–7*). A notable exception is contained in a paper by Gorring and de Rosset (*8*).

Many unsteady-state testing techniques involve arrays or groups of particles; these are normally in small packed beds and are commonly referred to as *chromatographic type tests*. Many models have been developed to describe such systems (*9–13*) and the tests are appealing in that they can be arranged so as to mimic closely the true conditions in which the porous solids will be used. The wealth of literature dealing with this testing technique is testimony to its popularity, but examination of the results produced shows that dispersion of a pulse of gas introduced into such beds is normally a weak function of the effective diffusivity within the porous solid itself. Gas-phase axial dispersion usually dominates as the pulse-spreading mechanism so that experimentally determined diffusivities are subject to large errors. In addition, as many as 10 unknown or inaccurately known parameters are involved in some of the models proposed to describe these tests; the method is perhaps best reserved for measuring axial dispersion rather than interparticle diffusion (*14*).

A promising variation on the chromatographic type tests is to employ a *single-pellet string reactor* (SPSR), as described, for instance, by Scott *et al.* (*15*). This consists of a tube, only slightly larger in diameter than the pellet, which is packed with upwards of 50 pellets. Provided the tube-to-particle diameter ratio lies between about 1.1 and 1.4, it appears that the SPSR

is in some respects equivalent to a packed bed of a more conventional aspect ratio; in particular, packed-bed correlations relating axial Peclet number to Reynolds number apply and a slightly modified Ergun equation adequately relates friction factors to superficial Reynolds numbers (*15–17*). High superficial velocities can be used without introducing intolerable pressure drops and the result is that experimental conditions can be manipulated so as to minimise the gas-phase axial dispersion term which normally contributes so dominantly to the spreading of a pulse of diffusing species as it traverses the bed. As a result it offers an attractive route for determining effective diffusion coefficients (*18*).

NOMENCLATURE

C_i	Inlet concentration to well-mixed volume
C_o	Outlet concentration from well-mixed volume
D_e	Effective diffusion coefficient
D_k	Knudsen diffusion coefficient
j_m	mth zero of J_0
J_0	Zero-order Bessel function, first kind
k	Shape factor defined by Eq. (2)
p	Radius-to-length ratio for cylinders
q	Volumetric flow rate
R_i, R_o	Inner or outer hollow cylinder radii
R	Characteristic length dimension, see Table 1
V_c	Well-mixed chamber volume surrounding the pellet
V_p	Envelope pellet volume
Y_0	Zero-order Bessel function, second kind
α_n	nth order unnormalised system moment about the origin $= \int_0^\infty t^n f(t)dt$
β_n	nth positive root of $[J_0(R_i\beta)Y_0(R_o\beta) - J_0(R_o\beta)Y_0(R_i\beta)] = 0$
ϵ	Pellet voidage
λ	Hollow cylinder radius ratio $= R_o/R_i$
τ	Tortuosity factor

THEORY

The basic theory behind our model has been presented elsewhere and therefore we only summarise it here (*19, 20*). A single particle of arbitrary shape resides in a well-mixed volume through which there is a constant volumetric flow rate of gas (Fig. 1). The concentration of a diffusing species in the inlet stream varies with time and this species diffuses freely into the pellet meeting negligible mass transfer resistance at the pellet surface; it neither reacts with, nor is adsorbed onto, the pellet surface. An equation for the behaviour of the well-mixed zone can be derived and linked with that describing diffusion within the pellet; this has been carried out for pellets of flat plate, spherical, cylindrical, or long hollow cylindrical form. In all cases the expressions for the first two system moments reduce to the following forms.

System mean

$$= \left[\frac{\alpha_1}{\alpha_0}\right] = \left[\frac{V_c + V_p\epsilon}{q}\right], \qquad (1)$$

System variance

$$= \left[\frac{\alpha_2}{\alpha_0} - \left(\frac{\alpha_1}{\alpha_0}\right)^2\right] = \left[\frac{V_c + V_p\epsilon}{q}\right]^2 + \frac{kV_p\epsilon^2R^2}{qD_e}. \qquad (2)$$

All symbols are defined under Nomenclature; in Eq. (2) the parameter k depends on the pellet geometry under study. In the case of a cylinder it is a function of the aspect ratio p, and for a long hollow cylinder it is dependent on the inside to outside radius ratio λ. The expressions for k are presented in Table 1 for common geometries; the quantity R in Eq. (2) is a particle characteristic length dimension and this is also specified in Table 1.

EXPERIMENTAL

The apparatus was built so as to conform as closely as possible with the conceptual model shown in Fig. 1. It was used to test a commercial catalyst, Hydronyl 356 GA 4C,

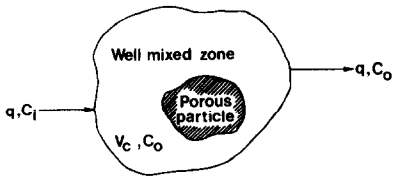

FIG. 1. Conceptual model of a porous particle in a well-mixed zone.

supplied by the Johnson Matthey Research Centre, Reading, England. The cylindrical catalyst pellets had an average diameter of 0.674 cm and an average length of 0.627 cm resulting in a pellet volume of just over 0.2 cm^3. In order to increase the relative contribution of the catalyst to the overall system response, cells were constructed to house several pellets. All results presented here are from a cell housing five pellets, each surrounded by a well-mixed volume. Conceptually the cell is equivalent to a series combination of five units, each one being as illustrated in Fig. 1. Means and variances are additive for noninteracting systems in series and this enables Eqs. (1) and (2) to be applied with all parameters relating to a single pellet provided the experimental mean and variance are first divided by 5. The well-mixed volume surrounding each pellet was 0.102 cm^3.

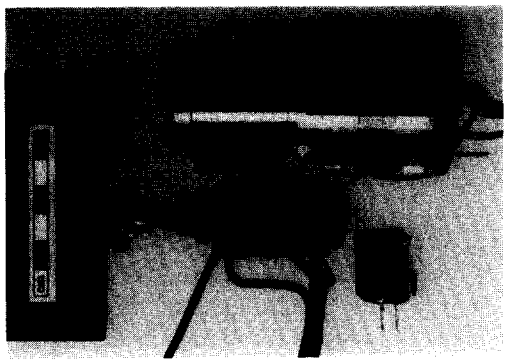

FIG. 2. Experimental apparatus showing catalyst test cell (centre top) bolted directly to the MK 158 microkatharometer. The eight-port gas changeover valve (centre) is driven by the solenoid (left) and produces a step change of the diffusing species. The switch to the right of the gas changeover value is triggered at the instant the step is produced and is used to activate the signal processing equipment.

The forcing function was a step change in concentration introduced into the inlet stream immediately before the test cell; the test cell was designed so that it could bolt directly onto a Taylor-Servomex MK 158 thermal conductivity detector, thus minimising delay times in transfer lines. This is seen in Fig. 2, which also shows the gas changeover valve used to produce the step, the solenoid which initiates the step, and the microswitch used to trigger the

TABLE 1

Characteristic Length Dimensions and Expressions for Shape Factors for Various Pellet Geometries

Pellet geometry	Length dimension R (see Eq. (2))	Unsteady-state shape factor k (see Eq. (2))
Flat plate	Plate thickness	1/6
Sphere	Radius	2/5
Cylinder		
(a) Full solution	Radius	$\frac{64}{\pi^2}\sum_{m=1}^{\infty}\sum_{n=0}^{\infty}\frac{1}{(2n+1)^2 j_m^2[j_m^2+(2n+1)^2p^2n^2]}$
(b) Ends sealed	Radius	1/4
(c) Sides sealed	Radius	$1/6p^2$
Hollow cylinder ends sealed	Wall thickness	$\frac{8}{(\lambda^2-1)(\lambda-1)^2}\sum_{n=0}^{\infty}\frac{1}{\beta_n^4}\frac{J_0(\beta_n)-J_0(\lambda\beta_n)}{J_0(\beta_n)+J_0(\lambda\beta_n)}$

signal processing circuit. The MK 158 detector has a time constant of the order of milliseconds for the flow rate ranges used and its linearity for all binary gas compositions ranging from pure nitrogen to pure argon was confirmed using the exponential dilution flask calibration technique due to Greco *et al.* (*21*).

There are particular advantages in using a step forcing function rather than an impulse and some of these are discussed below; however, the production of an ideal step change in concentration is not as simple as may be imagined and the following method was arrived at after a number of alternative designs had proved unsatisfactory. A conventional eight-port gas changeover valve (COV) was fitted with two identical "sample" coils of approximately 40 cm^3 volume each; these were made by coiling appropriate lengths of $\frac{1}{8}$-in. copper tubing and are illustrated diagrammatically in Fig. 3. At the start of the experiment the solenoid shown in Fig. 2 is activated, thus changing the COV position from A to B as illustrated in Fig. 3. By this means the coil containing argon is inserted in place of that containing nitrogen and provided the coil is sufficiently long, the transient test will be complete before the rear end of the argon slug reaches the catalyst test cell or detector. Steps produced in this manner were introduced directly into the inlet stream to the katharometer detecting chamber and the response of the detector monitored via the Servomex GC197 control unit on a storage oscilloscope. By these means it was determined that the elapsed time from the activation of the solenoid to the completion of the detector step response was less than 0.02 s. We should briefly discuss the rather unusual configuration in which the MK 158 katharometer was used. Conventionally a steady reference stream of unchanging composition would be taken to one chamber and the concentration of a second stream measured as a function of time relative to this reference; this is illustrated in Fig. 4A. In Fig. 4B we show the flow pattern which we adopted. In this latter configuration the step change is immediately detected by the first katharometer element and then the response from the catalyst test cell detected by the second element; thus the output from the katharometer following a step change is a closed pulse. By operating in this manner we are achieving zero-order dynamic compensation (*22*) and elsewhere (*5*) we have shown that this allows system moments to be evaluated by a sequence of signal integrations and subtractions. In particular, if the closed pulse step response is integrated directly, the final output of the integrator

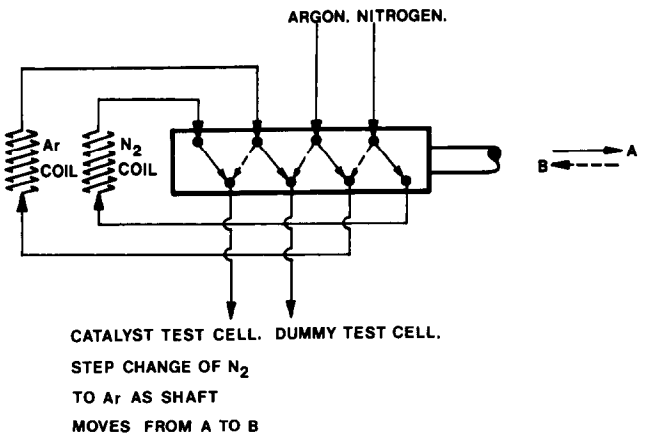

FIG. 3. Connections made to the gas changeover valve in order to produce the required step change in concentration.

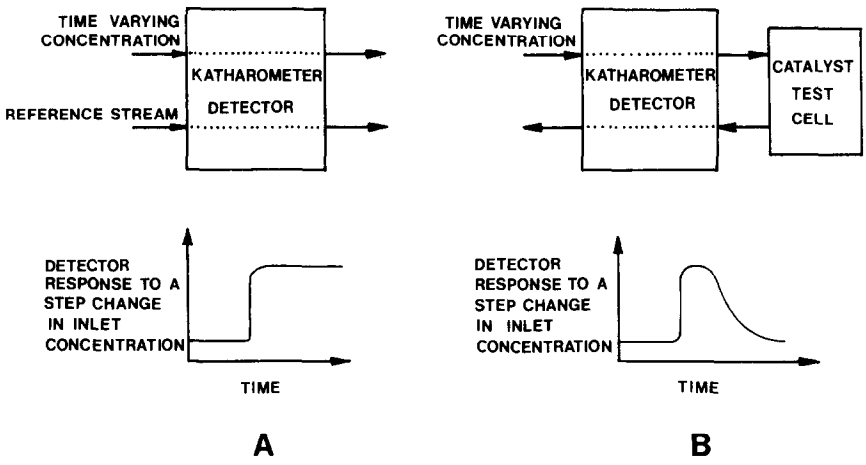

FIG. 4. (A) The conventional gas flow pattern for the MK 158 katharometer, together with step response. (B) The flow pattern which achieves zero-order compensation *in situ*, together with step response.

(i.e., the area under the pulse) will be the unnormalised first moment of the system residing between the two katharometer detecting elements; if dead volumes in piping can be made negligible and if the zeroth moment can be measured (the height of the conventional step response) then the system mean, α_1/α_0, can be evaluated and equated to the right-hand side of Eq. (1); the only unknown parameter, ϵ, the voidage, can thus be determined. Similarly, by subtracting the final value of the integrated step response (achieving first-order

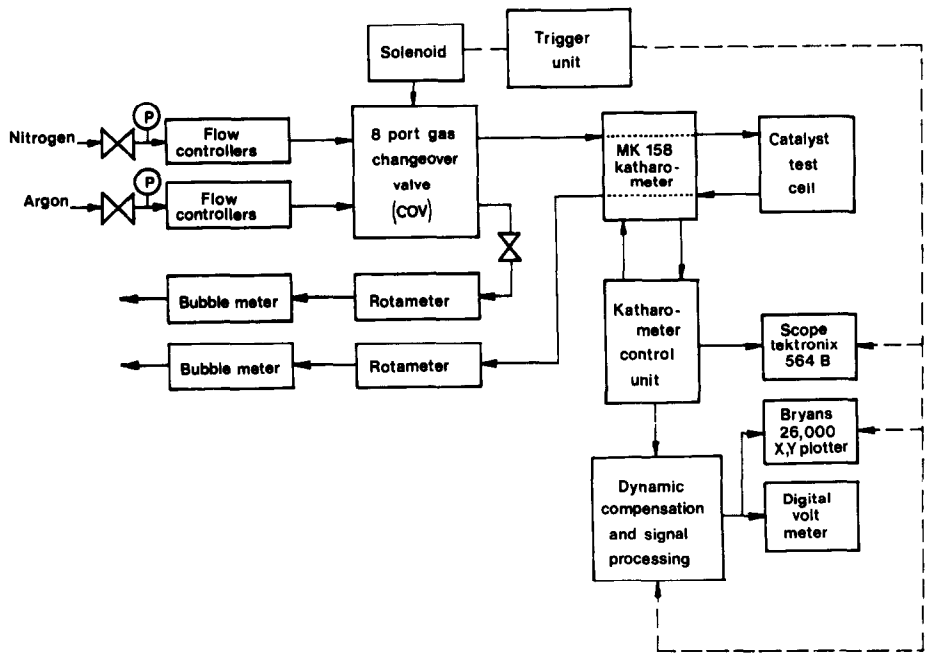

FIG. 5. Experimental layout.

compensation) and integrating a second time a value is obtained directly for α_2 the unnormalised second moment about the origin; this allows calculation of the variance and thus evaluation of D_e, the only unknown in Eq. (2). It should be appreciated that integration and subtraction of analogue signals can be carried out with great accuracy and speed using relatively simple analogue circuits. This means that moments can be evaluated in real time during the course of the transient test; for our systems the transients lasted for approximately 20 s. The need for data logging and off-line parameter extraction techniques is completely circumvented and a direct readout of the values of the moments on a digital voltmeter will clearly indicate when the contributions of the experimental curve to the moments are no longer significant in that the values will have converged to a steady reading. This incidentally does not happen until long after one would have judged visually that the transient was finished; typically we found the need to continue integrating for 15 to 20 system time constants. This observation emphasises that the response tail is vitally important in a diffusion test and that it contributes very significantly to the variance; accurate characterisation of the tail is of paramount importance.

Tests were conducted using the apparatus illustrated in Fig. 5. Dummy brass pellets of identical size and shape to the commercial catalyst were placed in the test cell and step responses monitored at different flow rates. The step responses should correspond to five well-mixed tanks in series (*23*) and this indeed was approximately so for flow rates in excess of 0.5 cm^3s^{-1}. This is illustrated in Fig. 6, where the plotted points are the experimental step response from the cell containing the five brass pellets when the throughflow was 0.533 cm^3s^{-1}. The experimentally determined system mean (the area under the response) is 0.978 s; ideally this figure should be five times the extrapellet volume

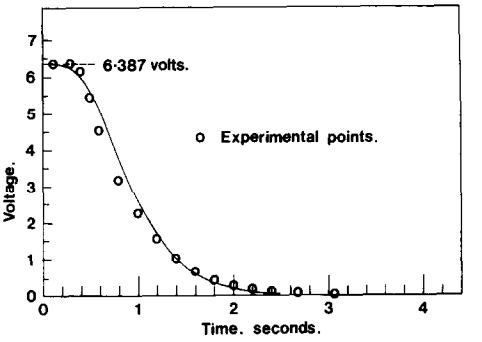

FIG. 6. Experimental zero-order compensated step response from the cell containing five brass pellets. The theoretical curve obtained by modelling the cell as five well-mixed volumes is also shown (solid line).

divided by the flow rate, i.e., 0.957 s. The fact that it is a little larger reflects a small contribution to the system volume of the lines linking the catalyst cell and the katharometer detector. Modelling the response of this system by that of five well-mixed volumes in series, each with a mean one-fifth of that determined experimentally (viz. 0.196 s), produces the solid line in Fig. 6; this shows acceptable agreement with the experimental points.

The variance of the experiment of Fig. 6 is the contribution to the general variance expression of Eq. (2) of everything other than the porous pellets; typically this is just under 0.2 s^2. For the data presented in Table 2 for the catalyst pellet tests, the lowest variance is 2.65 s^2, thus showing that even in the worst case over 90% of the system variance is contributed by the catalyst pellets themselves rather than surrounding gas volumes or inlet and outlet connections.

The ability of the five tanks in series model to describe the flow mixing pattern in the volumes surrounding the pellets was taken to indicate that negligible mass transfer resistance was present at the gas–solid interface, and this was verified independently by showing that experimentally determined diffusivities were independent of gas flow rate. In addition the correlation due to Petrovic and Thodos (*24*) indicated

TABLE 2

Experimental Readings and Derived Data

	α_0 (V)	α_1 (V · s)	α_2 (V · s²)	q (cm^3s^{-1})	ϵ	D_e (cm^2s^{-1})
Untreated pellets						
Test No. 1	6.516	10.43	37.88	0.719	0.572	0.0030
2	6.496	10.19	36.58	0.722	0.556	0.0029
3	6.516	10.43	37.86	0.719	0.573	0.0030
4	6.520	10.70	40.97	0.714	0.591	0.0029
Average values					0.573	0.0030
Pellets with sides sealed						
Test No. 1	6.469	9.669	56.79	0.714	0.498	0.0042
2	6.499	10.08	58.69	0.713	0.532	0.0047
3	6.502	10.04	55.10	0.714	0.529	0.0051
Average values					0.520	0.0047
Pellets with ends sealed						
Test No. 1	6.411	9.422	36.84	0.722	0.492	0.0034
2	6.396	9.316	33.84	0.723	0.485	0.0038
3	6.414	9.962	42.80	0.718	0.540	0.0034
4	6.412	8.859	29.22	0.723	0.437	0.0037
Average values					0.488	0.0036

negligible mass transfer resistance for the conditions used.

The whole pellet cell had an empty volume of 1.627 cm^3; with the brass pellets *in situ* this volume, minus the pellet volume, all divided by the volumetric flow rate, should equal the experimentally determined system mean. The total void volume within the cell was thus determined, with four independent readings giving volumes of 0.485, 0.521, 0.492, and 0.493 cm^3. The average of these is 0.498 cm^3 and enables the volume of the brass pellets to be determined as 1.129 cm^3; this agrees closely with direct physical measurements using a micrometer which gave a volume of 1.119 cm^3.

From a large batch of the alumina 356 GA 4C catalyst 50 pellets were selected as having virtually identical physical measurements. Diameters were 0.674 ± 0.0005 cm and lengths 0.627 ± 0.005 cm. Five pellets were introduced into the cell and a step response test conducted. This is shown in Fig. 7 which is a direct copy of the plot drawn on line by an x/y plotter. The step response is clearly seen as a closed pulse rising almost instantaneously to a maximum value of $\alpha_0 = 6.516$ V. The integral of this curve is also shown and clearly converges to a steady value of 10.43 V · s, the value of the first unnormalised moment. The form of the transient when first-order compensation is conducted is also shown, as is the integral of the latter which levels off at a steady value of 37.88 V · s^2, a direct measure of α_2. Knowing the values of the well-mixed chamber volume surrounding each pellet (0.102 cm^3), the volume of each pellet (0.224 cm^3), and the flow rate through the cell (0.719 cm^3s^{-1}) allows calculation of the pellet voidage from Eq. (1). Thus the voidage is 0.572.

This value for ϵ compared well with independent voidages of 0.595 evaluated from mercury porosimetry data, and 0.582 using air comparison pycnometry. Similarly Eq. (2) may be applied to evaluate the effective diffusion coefficient. In Eq. (2) k is the shape factor defined in Table 1; for p =

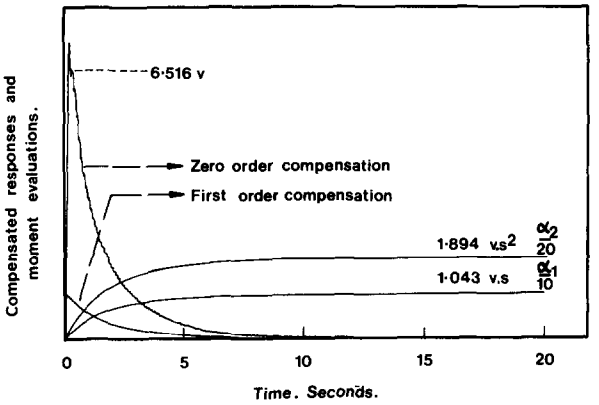

FIG. 7. Experimental step response with zero-order compensation. First-order compensation is also shown together with values for the first and second unnormalised system moments about the origin.

0.537 this assumes a value of 0.1436. Then $D_e = 0.0030\ cm^2s^{-1}$.

These results and those from three other tests on the same group of pellets are presented in Table 2.

The five pellets were now removed from the testing cell and sealed over their curved surface; this was achieved by coating the surface several times with a solution of Perspex in chloroform. Several other sealing methods were evaluated by investigating whether a pellet completely covered with sealant does behave as an inert object. The method described proved the most effective. Microscopic examination of the pellets sealed in this fashion revealed little apparent imbibition of sealing solution, though this observation was entirely qualitative.

Step response tests were now conducted with the five pellets sealed over their curved surface and the moments evaluated as previously. Diffusion is of course now in the axial direction and the results must thus be interpreted using the k value of $1/6p^2$ as specified in Table 1. Values of α_0, α_1, and α_2 for these tests together with a value for the volumetric flow rate at which they were observed are specified in Table 2; voidages and diffusivities calculated from three sets of independent readings are also presented.

Five other pellets were now sealed over their flat end faces and the tests repeated a third time; results for this case where diffusion is in the radial direction alone are also presented in Table 2.

DISCUSSION AND CONCLUSIONS

A technique has been described for measuring voidages and binary gas effective diffusion coefficients within porous pellets. Diffusion coefficients evaluated when diffusion is solely in the radial or axial directions can be measured without machining the pellet and these can be compared directly with whole pellet figures; in principle this allows gross pellet anisotropy to be detected.

Voidages for the alumina pellets as determined from the first system moment were in close agreement with independent measurements (0.57 vs 0.60 or 0.58). The average effective diffusion coefficient for the whole pellets was $0.0030\ cm^2s^{-1}$. Mercury porosimetry and nitrogen desorption were used to establish the pore size distribution which showed that the bulk of the pore volume was associated with pore diameters between 30 and 100 Å; diffusion can thus be expected to be largely in the Knudsen regime. A BET surface area measurement of $208\ m^2g^{-1}$ together with measurements of the voidage and pellet density allows an "average" pore radius to be defined and

this in turn, for a particular chemical species and specified temperature, specifies D_k the Knudsen diffusion coefficient (*25*). In our case this turned out to be 0.0090 cm^2s^{-1} for N_2 and 0.0108 cm^2s^{-1} for Ar at 25°C. Comparing the average of these figures with the mean whole pellet experimental figure indicates a value of ϵ/τ, the diffusibility of the solid, of 0.303. For the average voidage of 0.57 this corresponds to a tortuosity of 1.89 and is in general agreement with the data presented in Fig. 1.10 of Satterfield's text (*25*), and particularly the results of Villet and Wilhelm for silica–alumina commercial bead cracking catalyst (*26*).

The experimentally determined voidages for the pellets which have been partially sealed are lower than those for the untreated pellets by some 15%. This could be due to partial occlusion of the pellet voidage by the pellet sealing medium or alternatively could indicate that not all void spaces are interconnected thus preventing total access to all void spaces when approach is solely through the sides or ends of the pellets; either explanation seems quite reasonable.

Average values for the experimentally determined diffusivities are not radically different when they relate to diffusion tests involving the whole pellet or when they are for diffusion in the radial or axial direction alone. Certainly one would need to conduct many more experiments than presented in Table 2 before statistical significance could be attributed to the difference in experimentally determined diffusivities.

ACKNOWLEDGMENTS

The support of this work by the Science Research Council and the provision of catalyst samples by Johnson Matthey are gratefully acknowledged.

REFERENCES

1. Weisz, P. B., Prater, C. D., *in* "Advances in Catalysis and Related Subjects," Vol. 6, p. 143. Academic Press, New York/London, 1954.
2. Wicke, E., and Kallenbach, R., *Kolloid Z.* **97,** 135 (1941).
3. Weisz, P. B., *Z. Phys. Chem.* **11,** 1 (1957).
4. Gibilaro, L. G., Gioia, F., and Greco, G., Jr., *Chem. Eng. J.* **1,** 85 (1970).
5. Gibilaro, L. G., and Waldram, S. P., *Ind. Eng. Chem. Fund.* **12,** 472 (1973).
6. Moffat, A. J., *J. Catal.* **54,** 107 (1978).
7. Suzuki, M., and Smith, J. M., *AIChE J.* **18,** 326 (1972).
8. Gorring, R. L., and de Rosset, A. J., *J. Catal.* **3,** 341 (1964).
9. Aris, R., *Proc. Roy. Soc. Ser. A* **245,** 268 (1958).
10. Gunn, D. J., *Chem. Eng. Sci.* **25,** 53 (1970).
11. Haynes, H. W., Jr., *Chem. Eng. Sci.* **30,** 955 (1975).
12. Lighthill, M. J., and Whitham, G. B., *Proc. Roy. Soc. Ser. A* **229,** 281 (1955).
13. Suzuki, M., and Smith, J. M., *Chem. Eng. Sci.* **26,** 221 (1971).
14. Suzuki, M., and Smith, J. M., *Chem. Eng. J.* **3,** 256 (1972).
15. Scott, D. S., Wey, L., and Papa, J., *Chem. Eng. Sci.* **29,** 2155 (1974).
16. Haynes, H. W., Jr., *Chem. Eng. Sci.* **32,** 678 (1977).
17. Richardson, J. F., and Edwards, M. F., *Chem. Eng. Sci.* **23,** 109 (1968).
18. Cresswell, D. L., personal communication.
19. Greco, G., Jr., Iorio, G., Tola, G., and Waldram, S. P., *Trans. Inst. Chem. Eng.* **53,** 55 (1975).
20. Greco, G., Jr., Iorio, G., and Waldram, S. P., *Trans. Inst. Chem. Eng.* **54,** 199 (1976).
21. Greco, G., Jr., Gioia, F., Alfani. F., *La Chimica E L'Industria* **53,** 1133, (1971).
22. Gibilaro, L. G., and Waldram, S. P., *Chem. Eng. Sci.* **27,** 1569 (1972).
23. Levenspiel, O., "Chemical Reaction Engineering." Wiley, New York, 1972.
24. Petrovic, L. J., and Thodos, G., *Ind. Eng. Chem. Fund.* **7,** 274 (1968).
25. Satterfield, C. N., "Mass Transfer in Heterogeneous Catalysis." MIT Press, Cambridge, Mass., 1970.
26. Villet, R. H., and Wilhelm, R. H., *Ind. Eng. Chem.* **53,** 837 (1961).